



## Sorptive potential of glutaraldehyde cross-linked epoxyaminated chitosan for the removal of Pb(II) from aqueous media: kinetics and thermodynamic profile

Sreenivasan Rijith<sup>a</sup>, Thayyath Sreenivasan Anirudhan<sup>a,\*</sup>,  
Vijayakumari Sasidharan nair Sumi<sup>b</sup>, Thoudinja Shripathi<sup>c</sup>

<sup>a</sup>Department of Chemistry, University of Kerala, Kariavattom, Trivandrum 695 581, India, Tel. +91 9495538668; email: rijithsreenivas@gmail.com (S. Rijith), Tel. +91 4712418782; email: tsani@rediffmail.com (T.S. Anirudhan)

<sup>b</sup>Department of Chemistry, Government College, Attingal, Trivandrum, India, Tel. +91 9495538663; email: sumivvasi@rediffmail.com

<sup>c</sup>ESCA Lab and Molecular Spectroscopy LAB, UGC-DAE-CSR, University Campus, Khandawa Road, Indore 452017, India, Tel. +91 731 2463913; email: tshripathi@gmail.com

Received 29 November 2014; Accepted 29 June 2015

### ABSTRACT

In this study, the removal of Pb(II) ion from aqueous solutions by glutaraldehyde-cross-linked epoxyaminated chitosan (GA-C-ENCS) was investigated. The adsorbent (GA-C-ENCS) was characterized by FTIR, SEM-EDS, X-ray photoelectron spectroscopy, and potentiometric titration. Equilibrium sorption experiments were carried out at different operational conditions such as concentration, temperature, and pH values. Among the equilibrium studies the Langmuir isotherm model yields a much better fit than the Freundlich and Dubinin-Radushkevich models. The kinetics of sorption was investigated. The response time evaluation and batch adsorber design analysis was carried out using operational lines. Thermodynamic parameters reveal the spontaneous nature of sorption.

*Keywords:* Adsorption kinetics; Pb(II) removal; Chitosan; Thermodynamics; Counter current operation

### 1. Introduction

Heavy metal contamination of the aquatic environment has become an important issue with respect to environmental and human health. Long-term exposure of Pb(II) ion toward human health and natural ecosystems is a critical issue [1]. Lead is considered as a priority pollutant and major lead pollution has originated from the manufacture of storage batteries, painting pigments, ammunition, solder, plumbing fixtures,

radioactivity shields, auto mobiles, cable coverings, caulking, and bearings [2]. A large quantity of single or daily intake of lead can cause various disorders, such as damage to liver, kidney and reduction in hemoglobin formation, reproductive system, mental retardation, infertility and abnormalities in pregnant woman [3,4]. Pb(II) is regulated by USEPA with an action level of 15 µg/L in its drinking water regulations [5]. The problems caused by Pb(II) ion are curtailed by many physicochemical methods such as chemical reduction, ion-exchange, electrochemical

\*Corresponding author.

treatment, and adsorption [6]. Among these different physicochemical processes, sorption method has shown to be the best prospects owing to its economical feasibility, selective environment, cost effective, ease of operation and benign behavior [7]. For this purpose, numerous kinds of sorbents have been investigated and found useful, such as orange peel, marine algae, rice husk, coconut shell, wood and bark, sugar cane husk, and saw dust [8].

Chitosan has been used extensively as an adsorbent to treat water contaminated with toxic metals. In its original form, chitosan is a relatively weak base ( $pK_a \sim 6.2$ ) soluble in acidic media at  $pH < 6.0$ . Chemical modification of chitosan through cross-linking may be used to prevent the solubility when metal adsorption is performed in acidic solutions [9,10]. The metal binding capacity of the raw chitosan can be increased by grafting new functional groups onto chitosan backbone. Extensive studies involving the development of chitosan derivatives with new functional groups and their adsorption characteristics toward toxic metal ions have been reported in the literature [11,12].

The objective of this work was to explore the sorptive potential of surface-modified chitosan to remove Pb(II) ion from aqueous solutions. A simple chemical modification of cross-linking with glutaraldehyde followed by epichlorohydrin and ethylenediamine (transamidation) treatments was done to prevent the solubility of raw chitosan thereby increase the binding capacity. The preparation and characterization of the hybrid adsorbent were described, a series of adsorption experiments were carried out and kinetics and isotherms were investigated by fitting the experimental

data using different kinetic and isotherm models. The performance of this sorbent toward Pb(II) ion was investigated under various operating conditions such as pH, contact time, and temperature. The steady performance and robust nature of GA-C-ENCS were tested using regeneration studies.

## 2. Materials and methods

### 2.1. Materials

Chitosan (CS) (>90% deacetylation) was obtained from Central Institute of Fisheries Technology, Kochi (India). Stock solution of 1,000 mg/L Pb(II) was prepared by dissolving A.R. Grade anhydrous  $Pb(NO_3)_2$  in distilled water. All the working solutions with metal ion concentrations ranging from 25 to 600 mg/L were prepared by appropriate dilution of the stock solution using double distilled water. Epichlorohydrin (Fluka, Switzerland) was used as received. Glutaraldehyde (39%), HCl, NaOH, and  $H_2SO_4$  were procured from E. Merck (Worli, Mumbai, India). The pH of the working solutions was adjusted to desired concentration by the addition of 0.1 M HCl or 0.1 M NaOH solutions.

### 2.2. Preparation of adsorbent

The schematic diagram for the preparation of GA-C-ENCS is given in Fig. 1. Viscous CS solution was prepared by dissolving 3.0 g of CS in 2.0%, 200 mL of acetic acid and was pumped in to saturate caustic soda there by forming uniform beads. These

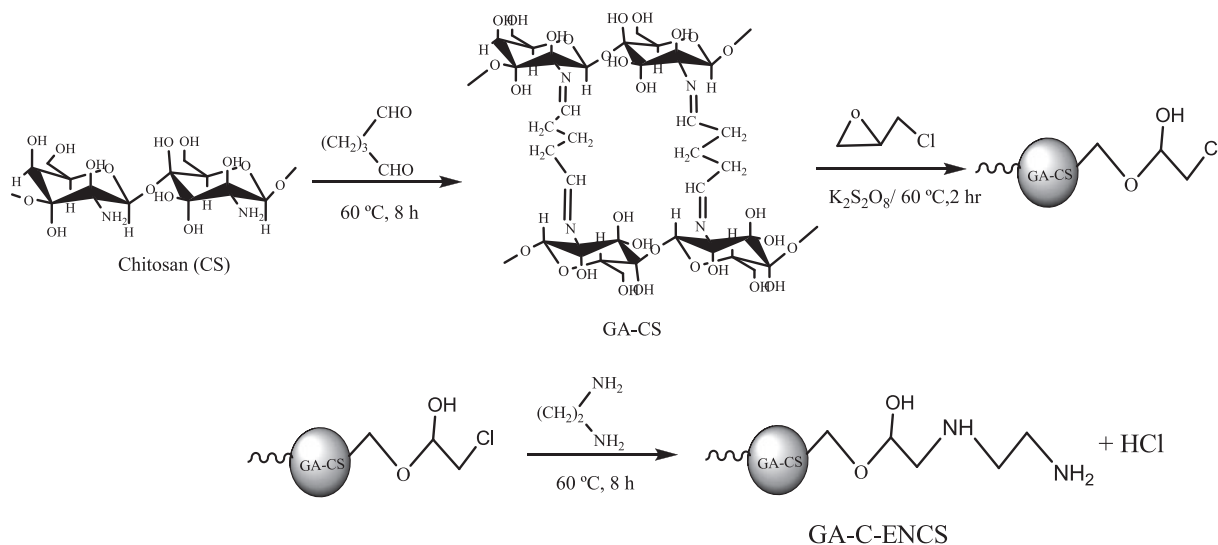


Fig. 1. Proposed mechanistic pathway for synthesis of GA-C-ENCS.

beads were washed with deionized water and dried. Chitosan–gluteraldehyde beads were prepared by suspending 25.0 g of the material in 0.05 M, 25 mL of gluteraldehyde solution heated at 60°C for 8 h. After 8 h, the cross-linked chitosan was washed with distilled water, filtered, and air-dried. The newly formed beads are called gluteraldehyde cross-linked chitosan beads (GA-C-CS).

About 15.0 g of cross-linked chitosan beads were functionalized by adding a mixture of epichlorohydrin and acetone (80 and 125 mL, respectively) in presence of 0.2 g of potassium persulfate (KPS) as initiator [13]. It was refluxed at a temperature of 60°C for 2 h. After 2 h, the beads were filtered, washed with acetone followed by amination with ethylene diamine (25 mL) to get gluteraldehyde cross-linked epoxyaminated chitosan. Hereafter, it is designated as GA-C-ENCS. It was oven dried, ground, and sieved using standard test sieves to approximate the particle diameter of 0.096 mm for conducting the batch experiments. The adsorbent with an average particle size of 0.096 mm was used for further adsorption experiments.

### 2.3. Equipments and method of characterization

In order to get a better understanding of the structural characteristics of CS, GA-C-CS, GA-C-ENCS, and Pb(II)-adsorbed GA-C-ENCS, detailed IR spectral studies were carried out. The IR spectra were recorded on a Shimadzu FTIR spectrophotometer model 1801 using pressed disk technique. Sample morphology and composition were observed and measured using a JSM-6390 scanning electron microscope (SEM) equipped with an INCA Energy 200 EDS-Microanalysis System. A potentiometric titration method was used to determine the pH of point of zero charge ( $\text{pH}_{\text{pzc}}$ ).

The  $\text{pH}_{\text{pzc}}$  determines the electrophoretic mobility where the net total surface charge density ( $\sigma_0$ ) is zero. The values of  $\sigma_0$  ( $\text{C cm}^{-2}$ ) were calculated from the titration curve using the following equation [14]:

$$\sigma_0 = F(\Gamma_{\text{H}^+} - \Gamma_{\text{OH}^-}) = \frac{F(C_A - C_B + [\text{OH}^-] - [\text{H}^+])}{A} \quad (1)$$

where  $F$  is the Faraday's constant, ( $\text{C/eq}$ ),  $\Gamma_{\text{H}^+}$ ,  $\Gamma_{\text{OH}^-}$  are the equivalent of  $\text{H}^+$  or  $\text{OH}^-$  bound to the suspension surface ( $\text{eq/cm}^2$ ),  $C_A, C_B$  are the concentrations of strong acid or strong base after each addition during titration ( $\text{eq/L}$ ).  $A$  is the surface area of the suspension ( $\text{cm}^2/\text{L}$ ). Potentiometric titration curves were obtained by plotting  $\sigma_0$  vs. pH of the suspension.

The X-ray photoelectron spectroscopy (XPS) analysis was carried out with an ESCALAB Mk II under the

conditions of high vacuum ( $10^{-7}$  Pa) Mg  $K\alpha$  radiation with energy of 1,253.6 eV was utilized. XPS peaks were decomposed into subcomponents using a Gaussian (80%)–Lorentzian (20%) curve fitting program, XPS peak fit, version 4.1 with a nonlinear background. A systronic microprocessor pH meter (model no. 362, India) was used to measure the potential and pH of the suspension. For kinetic and isotherm studies, a Labline (Labline Instruments Pvt. Ltd Kochi, India) temperature-controlled water bath shaker with a temperature tolerance of  $\pm 1.0^\circ\text{C}$  was used. The apparent density of the adsorbents was determined using specific gravity bottles. The absorbance measurement of Pb (II) solution were performed on a GBC Avanta A 5450 (Australia) Atomic Absorption Spectrometer.

### 2.4. Adsorption experiments

Batch adsorption experiments were performed to allow easy manipulation and measurement of process variables. Batch adsorption experiments were conducted using 100 mg of adsorbent with 50 mL of solutions containing Pb(II) ion of desired concentrations at different temperatures (20, 30, 40, and 50°C) and pH values (2.0–9.0) in 100 mL Erlenmeyer flasks. The pH of solutions was adjusted using 0.1 M HCl or 0.1 M NaOH solutions before adsorption analysis. For the adsorption isotherm experiments, the initial solution pH was 5.5, while the initial Pb(II) ion concentration in the solution varied between 50 and 500 mg/L. The flasks were shaken in a thermostatic shaker for 3 h with the mixing rate of 200 rpm and the solid phase was separated by centrifugation. The amount of metal ions sorbed at equilibrium,  $q_e$ , was calculated using the mass balance equation:

$$q_e = \frac{(C_0 - C_e)V}{m} \quad (2)$$

where  $C_0$  and  $C_e$  are the initial and equilibrium Pb(II) concentrations ( $\text{mg/L}$ ), respectively,  $m$  is the mass of GA-C ENCS (g) and  $V$  is the volume of the solution (L).

### 2.5. Desorption and regeneration studies

To investigate the possibility of regeneration of exhausted adsorbent is a critical consideration and contributor to process costs and recovery of metal ions. After performing adsorption experiments with 100 mg/L metal solution, the metal-loaded adsorbent was separated. The spent adsorbent was gently washed with distilled water to remove unadsorbed Pb

(II) ion. The exhausted adsorbent was added to desorption medium and shaken for 2 h to determine the amount of desorbed Pb(II) ion onto solution. The adsorbent was subjected to the subsequent Pb(II) loading cycle. The reusability of the adsorbent was further confirmed by repeating the adsorption–desorption cycle up to four times, thereby check out the long-term adsorption performance.

### 3. Results and discussion

#### 3.1. Adsorbent characterization

The IR spectra of CS, GA-C-CS, GA-C-ENCS, and Pb(II)-GA-C-ENCS are shown in Fig. 2. The spectrum of pure CS shows peak around at  $3,450\text{ cm}^{-1}$  corresponding to amine N–H symmetrical vibration and H bonded –OH group in CS. The peaks present on the range  $3,400\text{--}3,800\text{ cm}^{-1}$  also indicate the –OH and –NH<sub>2</sub> moieties in the CS backbone. The intense peaks at  $2,890$  and  $2,320\text{ cm}^{-1}$  are assigned to the symmetric and asymmetric –CH<sub>2</sub> vibrations of carbohydrate ring. The CS spectrum also shows the distinctive absorption peak at  $1,650\text{ cm}^{-1}$  (–C=O in amide group, amide I vibration),  $1,561\text{ cm}^{-1}$  (–NH<sub>2</sub> bonding in non-acetylated 2-aminoglucose primary amine, amide II vibration), and  $1,392\text{ cm}^{-1}$  (–N–H stretching or C–N bond stretching vibrations, amide III vibration). The peak at  $1,091.7\text{ cm}^{-1}$  corresponds to the symmetric stretching of –C–O–C– groups. The absorption peaks in the range  $900\text{--}1,100\text{ cm}^{-1}$  are due to the antisymmetric –C–O stretching from the pyranose ring and wagging of saccharide structure of CS. The spectrum of GA-C-CS exhibits many alternations. The wide absorption band at  $3,413.65\text{ cm}^{-1}$  in CS, corresponding to the stretching vibration of –NH<sub>2</sub> group and –OH group, shows a significant change to higher wave number ( $3,430.14\text{ cm}^{-1}$ ). The peaks found at  $2,868.13$  and  $1,659.16\text{ cm}^{-1}$  were attributed to the C–H stretching from secondary alcoholic groups and C=N stretching from imine groups, respectively, which clearly indicates the cross-linking occurred on the NH<sub>2</sub> groups in CS. The illustrative peak at  $3,430.14\text{ cm}^{-1}$  for GA-C-CS was disappeared after treatment with epichlorohydrin followed by amination. This indicates that the secondary alcoholic groups were involved in radical initiated chain propagation.

GA-C-ENCS also shows predominant peaks at  $3,279.8$  and  $1,563.4\text{ cm}^{-1}$  assign the N–H stretching from secondary amine linkage on the surface. The peak at  $1,050\text{ cm}^{-1}$  assigned to skeletal vibration involving stretching of both C–O and C–C bonds attached to the glycosidic linkage [15]. There are no significant changes on the peaks observed in the range

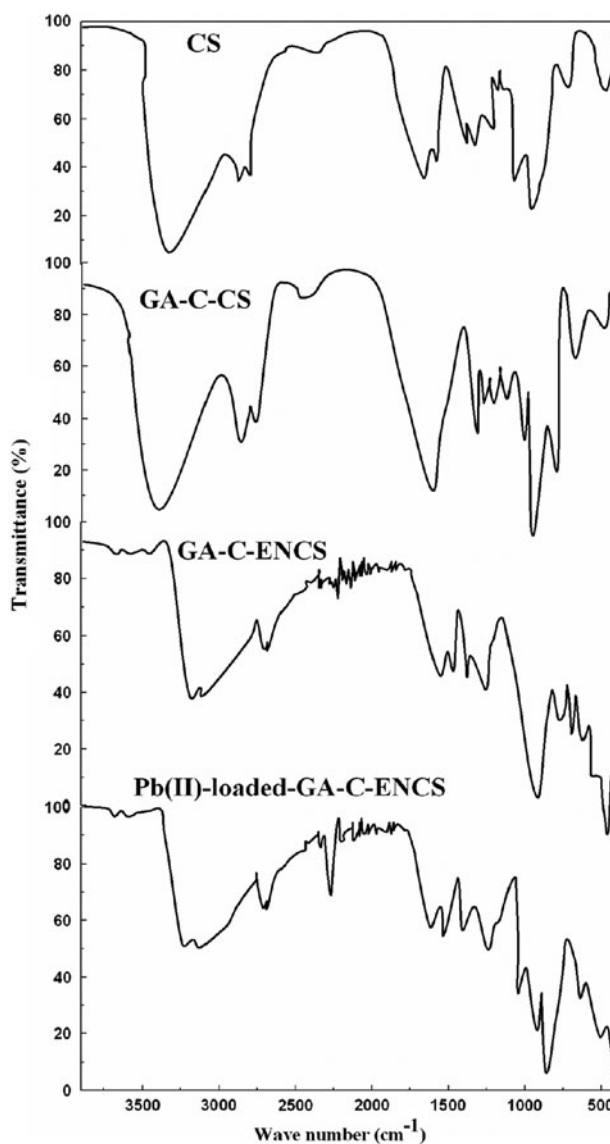


Fig. 2. FTIR spectra of CS, GA-C-CS, GA-C-ENCS, and Pb(II)-GA-C-ENCS.

$920\text{--}1,200\text{ cm}^{-1}$  which clearly shows that ethereal linkage was not ruptured during cross-linking as well as radical initiated chain propagation. The peak found at  $3,279.8\text{ cm}^{-1}$  in GA-C-ENCS was slightly shifted to  $3,285.5\text{ cm}^{-1}$  and the peak at  $2,365.8\text{ cm}^{-1}$ , which indicate the metal coordinated –NH stretching vibration.

Fig. 2 also represent the changes occur in the spectrum of GA-C-ENCS after sorption of Pb(II). The peak intensity at  $1,650\text{--}1,660\text{ cm}^{-1}$  of metal-loaded GA-C-ENCS, corresponds to the superimposition of different amide I band (C–O stretching coupled with N–H deformation mode) and it was significantly decreased after the complexation of metal ions with the functional groups on the surfaces of GA-C-ENCS.

When the GA-C-ENCS was loaded with the Pb(II) ion, the peaks at 1,455 and 1,306  $\text{cm}^{-1}$  in GA-C-ENCS were not altered, so it led to the conclusion that during the sorption process the C–O–C bond in the polysaccharidic residues was not ruptured. Furthermore, the formation of hydrogen bond between the amino group and metal ion is indicated by the appearance of an additional peak shoulder at 879  $\text{cm}^{-1}$  in the Pb(II)-GA-C-ENCS.

After metal sorption, the peak intensity decreases with band shifts at the lower wave numbers (under 700  $\text{cm}^{-1}$ ) indicates the interaction between metal ions and nitrogenous functional groups on the surface of GA-C-ENCS. From these spectra, the sorption of Pb(II) onto GA-C-ENCS primarily follow through the complexation with amine moieties on the surface.

The SEM images of GA-C-ENCS, and Pb(II)-GA-C-ENCS are shown in Fig. 3. SEM images illustrate

entirely different morphological structure for GA-C-ENCS and the sorbent surface was aligned in a nonuniform and irregular way to form many porous ridges. GA-C-ENCS shows several irregular cavities with a certain surface porosity. These microstructures showed a drastic change after GA-C-ENCS was sorbed with Pb(II). This observation provides evidence that Pb(II) was loaded onto GA-C-ENCS not only the surface functional moieties but also located underneath the sorbent surface. The dried Pb(II)-loaded-GA-C-ENCS shows that the Pb(II) ion are randomly distributes the sorbent surface and the holes were used as growing nucleus. The EDS analysis (Fig. 3) provided a rudimentary composition for the GA-C-ENCS and Pb(II)-GA-C-ENCS. It was found that carbon, nitrogen, and oxygen were the only consistent components in the GA-C-ENCS and Pb(II)-loaded-GA-C-ENCS which clearly indicate that the metal ions

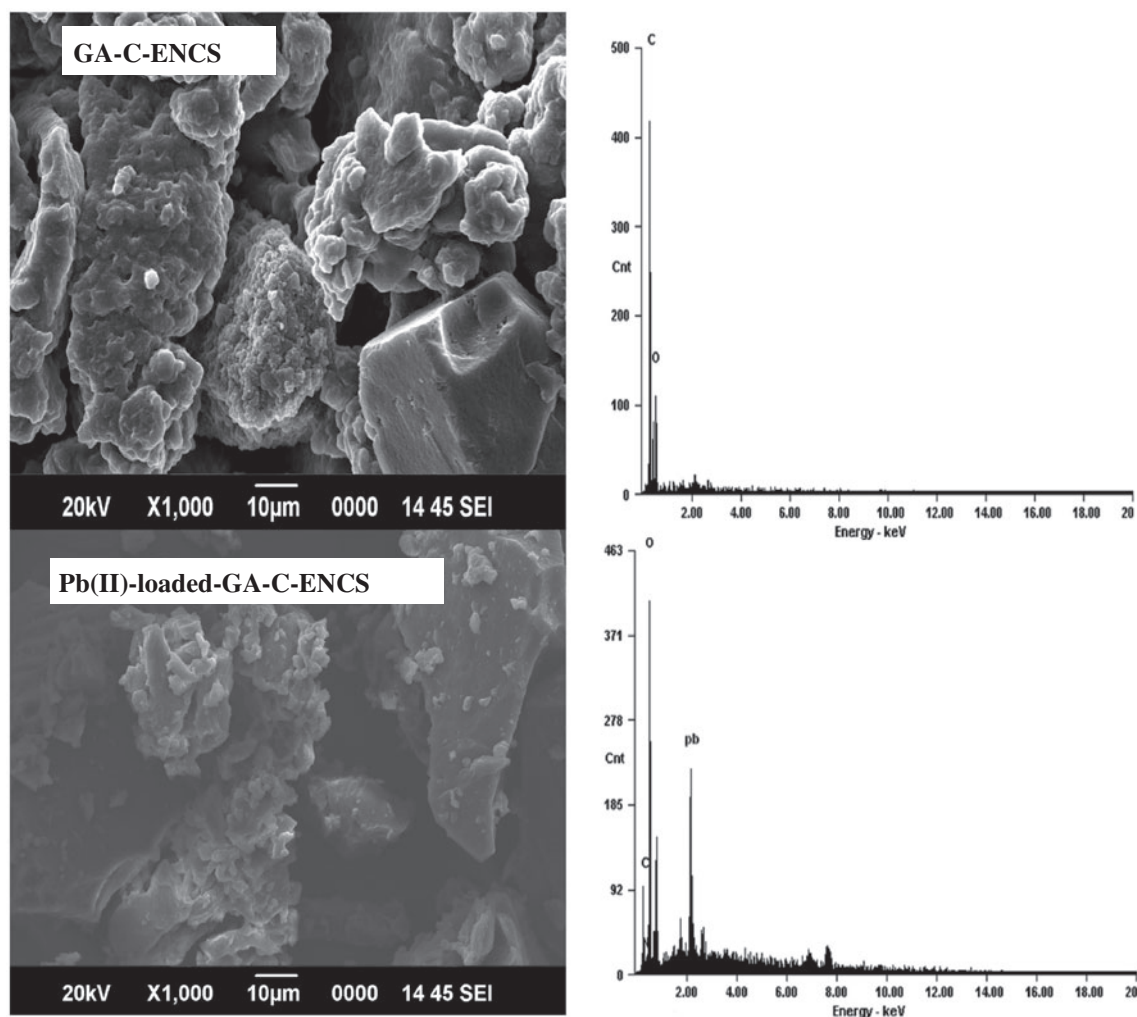


Fig. 3. SEM and EDS images of GA-C-ENCS, and Pb(II)-GA-C-ENCS.

were distributed on the surface of GA-C-ENCS. SEM-EDS images also revealed that the GA-C-ENCS was enriched with Pb(II) ion after sorption process. The EDS spectra give the significant amount of metal loading after the adsorption of Pb(II) ion. To further verify the findings from the above-mentioned spectral

studies, XPS analysis was employed. XPS spectra have widely been used to identify the existence of a particular element and to distinguish the different forms of the same element in a material. To further understand the sorption mechanism of Pb(II) onto GA-C-ENCS, binding energy values of GA-C-ENCS

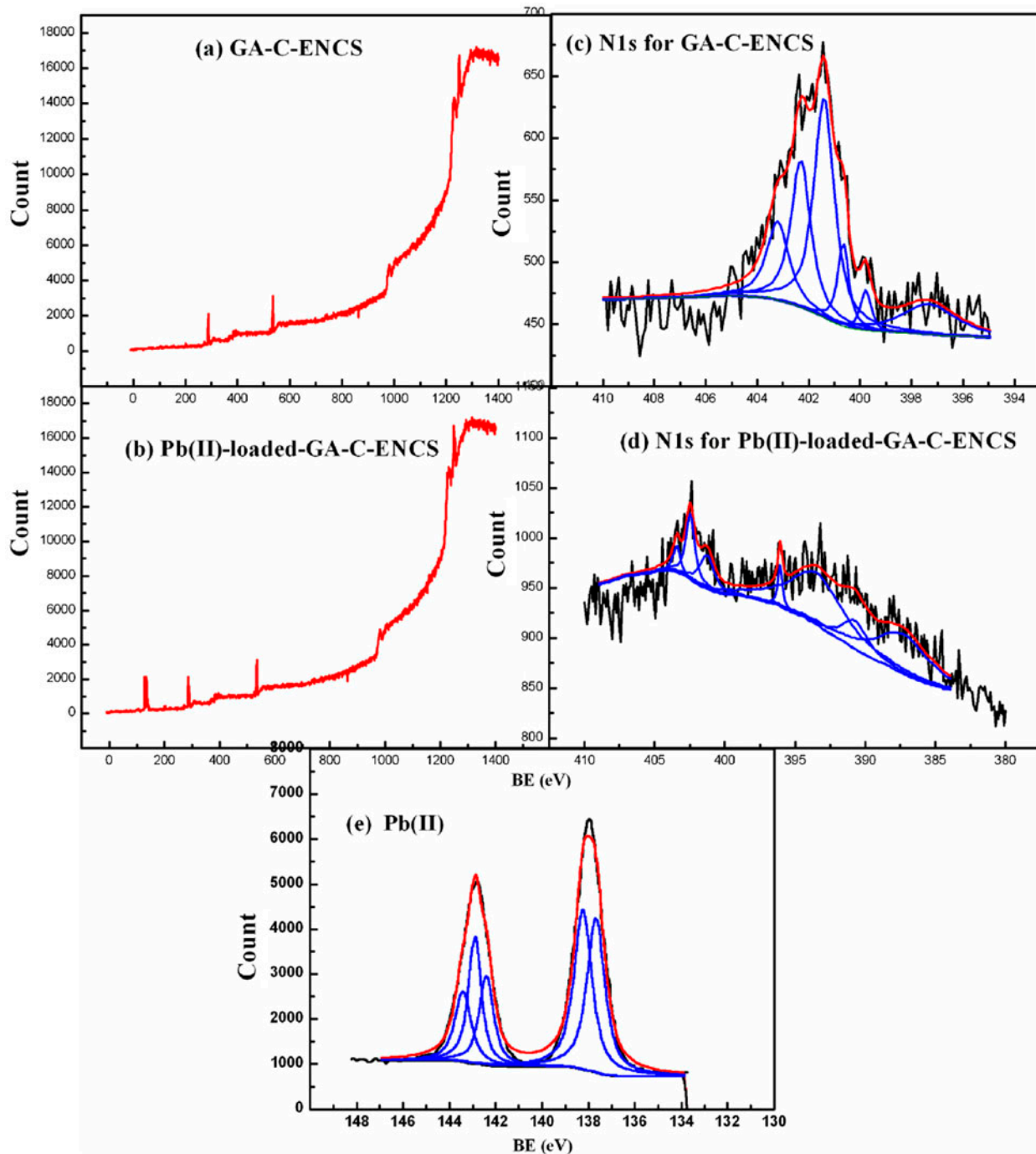


Fig. 4. XPS full scans for GA-C-ENCS (a), Pb(II)-GA-C-ENCS (b), deconvoluted high resolution scans of N1s for GA-C-ENCS (c), N1s for Pb(II)-GA-C-ENCS (d), and (e) Pb4f.

and Pb(II)-GA-C-ENCS were measured by XPS and their results are shown in Fig. 4. It also gave an overview of the chemical composition of samples analyzed based on the XPS survey scans.

The XPS survey scan of GA-C-ENCS indicate the BE peaks characteristics of C1s, O1s, and N1s ranges 280–290 eV, 510–540 eV, and 385–405 eV, respectively. In addition to the said peaks, the spectrum of Pb(II)-GA-C-ENCS also shows satellite peak at a range of 135–145 eV for Pb(II) species. The N1s core-level spectrum of GA-C-ENCS show the peaks at the binding energy (BE) of 399.2 and 401.0 eV ((Fig. 4(d)) corresponding to the N–H stretching in the neutral amine ( $-\text{NH}_2$  or  $-\text{NH}-$ ) and protonated amine ( $-\text{NH}_3^+$  or  $-\text{NH}_2^+$ ), respectively [16]. After the adsorption of Pb(II) on GA-C-ENCS, the N1s spectrum of Pb(II)-GA-C-ENCS (Fig. 4(d)) shows multiple (satellites) peaks. The new peak appeared at the binding energy range 400–402 eV ascribed the nitrogen coordinated to heavy metal ion (i.e. in  $-\text{NH}_2-\text{Pb(II)}$  or  $=\text{NH}-\text{Pb(II)}$ ), which indicate the nitrogen in the neutral amines existing in a more oxidized state and hence had a higher BE [17].

High-resolution Pb4f spectra of the GA-C-ENCS after Pb(II) uptake are shown in Fig. 4(e). The XPS Pb4f spectrum (Fig. 4(e)) of Pb(II)-GA-C-ENCS) shows a doublet characteristics of Pb(II) appeared at 138.2 eV (assigned to  $\text{Pb}4f_{7/2}$ ) and 142.9 eV (assigned to  $\text{Pb}4f_{3/2}$ ). The binding energy of  $\text{Pb}4f_{7/2}$  of Pb(II) species was found to be in the range 139.1–139.5 eV [18], and the

significant chemical shift was assigned to the interaction of  $\text{Pb}^{2+}$  with GA-C-ENCS. The reduced value of area ratio was consistent with the intended  $\text{Pb}^{2+}$ -amine groups on the surface of chain backbone of GA-C-ENCS in 1:2 molar ratio. This is consistent with the observations in both sorption isotherm and kinetic experiments.

### 3.2. Effect of pH on metal sorption

Experiments were conducted to determine the optimum pH for the metal uptake onto GA-C-ENCS by varying pH (2.0–9.0) with 50 and 100 mg/L initial concentrations and the results are presented in Fig. 5. All experiments were conducted at pH values below the onset of metal hydrolysis and precipitation, estimated as  $\text{pH} < 6.3$  [19]. Since the amino groups on the adsorbent surface get protonated at very low pHs, the electrostatic interaction between the adsorbent surface and the  $\text{Pb}^{2+}$  ions to be adsorbed is electrostatically repulsive as  $\text{Pb}^{2+}$  ions were the major species in the solution. This electrostatic repulsion prevented Pb(II) ion from the reaction sites, resulting in a decreased metal uptake at very low pHs.

The fractional distribution of metal ions with pH [20–22] are also depicted in Fig. 5. From the speciation diagram, the chemical precipitation of metal hydroxide occurs above  $\text{pH} 6.0$ . The speciation also shows that  $\text{Pb}^{2+}$  was the prevailing species only at the pH

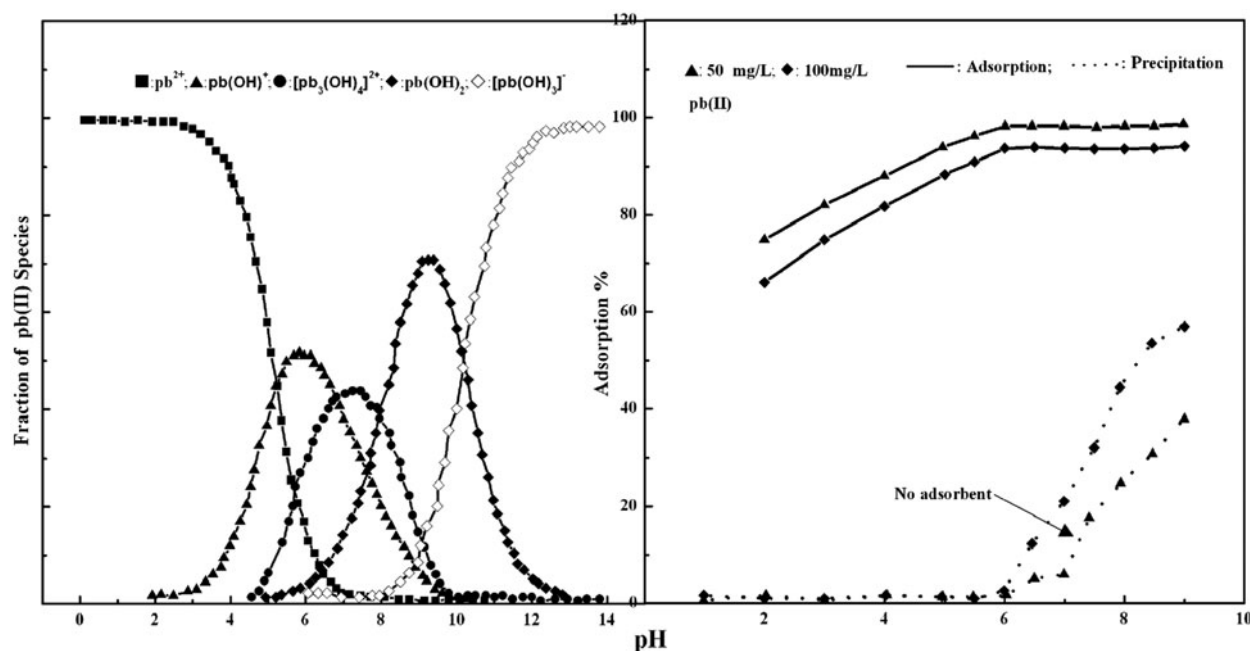


Fig. 5. Effect of pH on the removal of Pb(II) on GA-C-ENCS and the speciation of Pb(II) species.

below 6.0. Experimental results shows that the maximum adsorption for Pb(II) observed at a pH range 6.0–7.0. With an increase in pH of the solution from 2.0 to 6.0, the removal capacity increased from 75.0 to 98.9% and 63.0 to 83.2% at an initial Pb(II) concentration of 50 and 100 mg/L, respectively.

The  $pH_{pzc}$  of the GA-C-ENCS was found to be 5.8 and below this pH, surface charge of the sorbent is positive. At below pH 5.2, the amine moieties present in the surface of GA-C-ENCS become protonated. As a result of this protonation and the competition between the protons and metal ion species inhibit the adsorption of positively charged metal ion onto GA-C-ENCS. In high acidic solutions, higher competitions exist between divalent metal ion species with the protons for the sorption sites thereby decline the uptake capacity. An increase in pH above  $pH_{pzc}$  shows the increase in adsorption trend due to the increase in surface negative charge. As the surface become negatively charged, which enhance the electrostatic attraction between the positive metallic species and adsorbent particles lead to increase in adsorption. The stable trend was observed in the adsorption of Pb(II) onto GA-C-ENCS at higher pH values (>6.0) indicates the sorption of divalent Pb(II) species with the amine moieties on the surface of GA-C-ENCS.

### 3.3. Effect of contact time and initial concentration

The most important parameters that define adsorbent are adsorption time and adsorption capacity. Adsorption time defines the efficiency of adsorption and it helps to determine effluent uptake rate through a batch reactor for optimal removal of a particular contaminant. Fig. 6 shows the effect of contact time on the adsorption of Pb(II) onto GA-C-ENCS. The sorption capacity increases very rapidly up to 30 min and slowly reaches saturation at about 2 h. Depending on the initial concentrations about 70–80% removal of Pb(II) species was achieved during the first 30 min of the contact time, whereas only 15–20% of additional removal occurred within 2 h of contact time. There is no significant influence of contact time on the adsorption efficiency after a contact time of 2 h. The equilibrium time of 2 h can be considered very short, which is an economically favorable condition for the adsorbent described here. The uptake (removal efficiency) of Pb(II) after equilibrium was found to be 43.02 mg/g (86.04%), 69.01 mg/g (92.01%), 87.45 mg/g (87.45%), and 112.93 mg/g (90.34%), respectively, for an initial concentration of 100, 150, 200, and 250 mg/L.

The results show that an increase in the initial Pb(II) concentration leads to a decrease in the metal uptake. The important driving force to overcome all

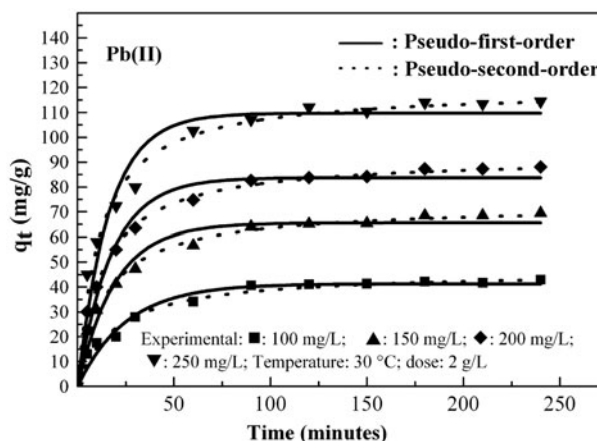


Fig. 6. Effect of initial concentration and contact time on the adsorption of Pb(II) onto GA-C-ENCS and comparison of observed data with pseudo-first-order and pseudo-second-order kinetic model.

mass transfer resistance between solid–liquid phases was the initial concentration of adsorbed species. Hence, a higher initial Pb(II) concentration would retard the sorption process. Similar trend was observed in the sorption of Pb(II) onto GA-C-ENCS, and it was illustrated in Table 1.

At low initial concentration, the ratio of initial number of moles of metal ions to the available adsorption sites is low and subsequently the fractional adsorption becomes independent of initial concentration. However, at higher concentration, the available sites of adsorption become fewer due to monolayer formation and hence the percentage removal of metal ions depends upon the initial concentration. The amount of metal ions is relatively higher as compared to availability of binding sites at higher metal ion concentration. Due to restriction of binding sites present on the surface of GA-C-ENCS, adsorbent becomes saturated at higher initial concentrations. After lapse of some time, the remaining vacant surface sites are difficult to be occupied due to repulsive forces from metal ionic species adsorbed on GA-C-ENCS surface. Here, the active surface sites get almost saturated. Thereafter, metal ions have to traverse farther and deeper into the active intra-particle sites encountering much larger resistance. This slows down the rate of metal adsorption during later period of adsorption.

### 3.4. Adsorption kinetics

The prediction of sorption rate gives important information for designing batch adsorption systems. Information on the kinetics of solute uptake is required for selecting optimum operating conditions

Table 1  
Kinetic parameters for the adsorption of Pb(II) onto GA-C-ENCS at different concentrations

Concentration (mg/L)	Pseudo-first-order					Pseudo-second-order				
	$q_{e,exp}$ (mg/g)	$k_1 \times 10^{-2}$ (min <sup>-1</sup> )	$q_{e,cal}$ (mg/g)	$R^2$	$\chi^2$	$k_2 \times 10^{-2}$ (g/mg/min)	$q_{e,cal}$ (mg/g)	$R^2$	$\chi^2$	
100	43.02	3.97	39.24	0.96	9.90	1.12	43.29	0.99	4.21	
150	69.01	5.21	65.55	0.96	21.31	0.97	72.59	0.99	3.25	
200	87.45	5.75	83.69	0.97	28.04	0.86	92.14	0.99	3.24	
250	112.93	6.20	109.66	0.95	62.25	0.76	114.43	0.99	2.21	

for full-scale batch process [23]. The kinetic parameters for the adsorption of Pb(II) onto GA-C-ENCS were evaluated using Lagergren pseudo-first-order and pseudo-second-order equations:

$$\text{Pseudo-first-order model: } q_t = q_e(1 - e^{-k_1 t}) \quad (3)$$

$$\text{Pseudo-second-order model: } q_e = \frac{k_2 q_e^2 t}{1 + k_2 q_e t} \quad (4)$$

The pseudo-first-order rate constant  $k_1$  and pseudo-second-order rate constant  $k_2$  were obtained from nonlinear regression analysis. The experimental kinetic data are fitted using the kinetic model described above and the values obtained were depicted in Table 1. The values of  $k_1$  were found to be increased from  $3.97 \times 10^{-2}$  to  $6.20 \times 10^{-2}$  for Pb(II) at an initial concentration from 100 to 250 mg/L. The adsorption kinetics was best described by Lagergren model for the first 30 min and thereafter the data deviate from theory, so this equation was not valid for the entire sorption process. This confirms that this model is inappropriate to predict the sorption kinetics. From the regression coefficients and chi-square values depict that Lagergren model gave poor fit between the calculated and experimental  $q_e$  values.

The experimental data and model predicted data from the pseudo-second-order models gave better fit over the entire sorption process (Table 1). The theoretical  $q_e$  values estimated from the pseudo-second-order model gave almost similar values compared to the experimental values. The correlation coefficients are greater than 0.99 and the reduced chi-square values indicating the applicability of this kinetic equation and the sorption phenomena followed the pseudo-second-order kinetics for the entire sorption process. The decrease in pseudo-second-order rate constant ( $k_2$ ) values with increasing concentration indicated the metal adsorption on GA-C-ENCS is becoming faster with increasing the solute concentration in solution.

The above-said methods cannot sufficient to interpret the sorption mechanism. In order to understand the behavior of the static sorption process, Pb(II) sorption data were analyzed using first-order-reversible kinetic model. The kinetic equation employed to study the sorption process was depicted as:

$$\text{Reversible-first-order: } \ln\left(1 - \frac{X_A}{X_{Ae}}\right) = -(k_1 + k_2)t = -k't \quad (5)$$

where  $k_1$ ,  $k_2$ , and  $k'$  are the forward reaction rate constant, the backward reaction rate constant and the overall rate constant.  $X_A$  and  $X_{Ae}$  are the concentration of metal species adsorbed at time “ $t$ ” and equilibrium, respectively. By plotting  $-\ln(1 - X_A/X_{Ae})$  vs.  $t$  (Fig. 7) illustrates the sorption behavior from the first-order forward and backward rate constants obtained. The linearity of this kinetic model with the data obtained by all the sorption process of metal ions toward GA-C-ENCS was moderate fit. From Table 2, the

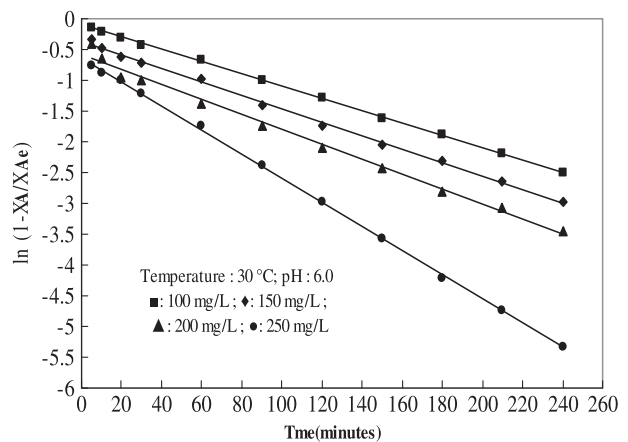


Fig. 7. Reversible-first-order kinetic plots for the adsorption of Pb(II) onto GA-C-ENCS.

Table 2

Kinetic parameters for the adsorption of Pb(II) onto GA-C-ENCS at different concentrations

Conc. (mg/L)	Reversible-first-order					$R^2$
	$q_{e,exp}$ (mg/g)	$k_1 \times 10^{-2}$ (min <sup>-1</sup> )	$k_2 \times 10^{-2}$ (min <sup>-1</sup> )	$k'$	$\Gamma_{resp}$ (min)	
100	43.02	0.81	0.23	1.04	96.10	0.98
150	69.01	0.82	0.29	1.11	90.10	0.99
200	87.45	0.88	0.34	1.22	91.97	0.97
250	112.93	1.32	0.64	1.96	51.02	0.98

overall rate constants for the sorption of Pb(II) was also increased from  $1.04 \times 10^{-2}$  to  $1.96 \times 10^{-2}$  with the faster forward reaction step. The rate of forward reaction,  $k_1$ , was faster than that of the backward reaction (desorption process),  $k_2$ , at all the concentrations studied. The system response time ( $\Gamma_{resp}$ ), defined as the reciprocal of the overall rate constant, was used to evaluate concentration dependence to attain equilibrium.

$$\Gamma_{resp} = \frac{1}{k_1 + k_2} \quad (6)$$

$\Gamma_{resp}$ , representing the time required for the system to reach the new equilibrium with varying concentration [24]. When the initial metal ion concentration increased from 100 to 250 mg/L,  $\Gamma_{resp}$  was found to decrease from 96.01 to 51.02 min for the sorption of Pb (II) onto GA-C-ENCS. This revealed that the new equilibrium at higher initial concentration could be ascribed to the increase in the driving force of overcoming all mass transfer resistance between the metal ion moieties and the GA-C-ENCS with the increase in the initial concentration. This indicates the extent of adsorption decrease with increase in concentration. The magnitude of change in forward rate constant is not equal to that of change in backward rate constant with varying concentration. Decreasing tendency of response time with increase in concentration indicates the competition of sorbate toward binding sites, which reduces the sorption potential.

### 3.5. Adsorption isotherm study

Adsorption isotherm provides an approximate estimation of the adsorption capacity of the adsorbent. Adsorption isotherm is very important as it provides the framework for describing the extent and strength of adsorption of molecules on surface. Thus, the correlation of equilibrium data using a theoretical or

an empirical model is essential for interpreting the sorption process. Among the several well-known isotherm models, three of them are used here to interpret the equilibrium data. Three widely used models such as Langmuir, Freundlich, and Dubinin–Radushkevich are employed here. All the isotherm data were interpreted using the nonlinear forms of these models.

Experimental isotherm data of Pb(II) adsorption onto GA-C-ENCS at different temperatures are shown in Fig. 8. As shown in figure, the adsorbed amount increased with increase in concentration of metal ions. The nonlinear Langmuir, Freundlich, and Dubinin–Radushkevich (D–R) adsorption isotherm models were applied to analyze the experimental data. From reduced chi-square values, interpret which model gave better fit at the equilibrium sorption process.

The nonlinear Langmuir equation is given by the following relation:

$$q_e = \frac{Q_0 b C_e}{1 + b C_e} \quad (7)$$

where  $q_e$  and  $C_e$  are the amount adsorbed (mg/g) and sorbate concentration in solution (mg/L), both at equilibrium.  $Q_0$  and  $b$  are the Langmuir constants related to monolayer adsorption capacity and energy of adsorption, respectively. The Langmuir model is applicable to homogeneous adsorption, where the adsorption of each molecule onto the surface has equal adsorption activation energy. The values of  $Q_0$  increased from 145.76 to 166.75 mg/L when the temperature increased from 20 to 50°C, while the values of  $b$  increased from 0.05 to 0.09 L/mg. This indicates that Pb(II) adsorption capacity on GA-C-ENCS and intensity of adsorption were enhanced at higher temperatures. The Freundlich isotherm is an empirical model and can be used to describe the sorption on heterogeneous surfaces as well as multilayer sorption. The nonlinear Freundlich equation is given below:

$$q_e = K_F C_e^{1/n_F} \quad (8)$$

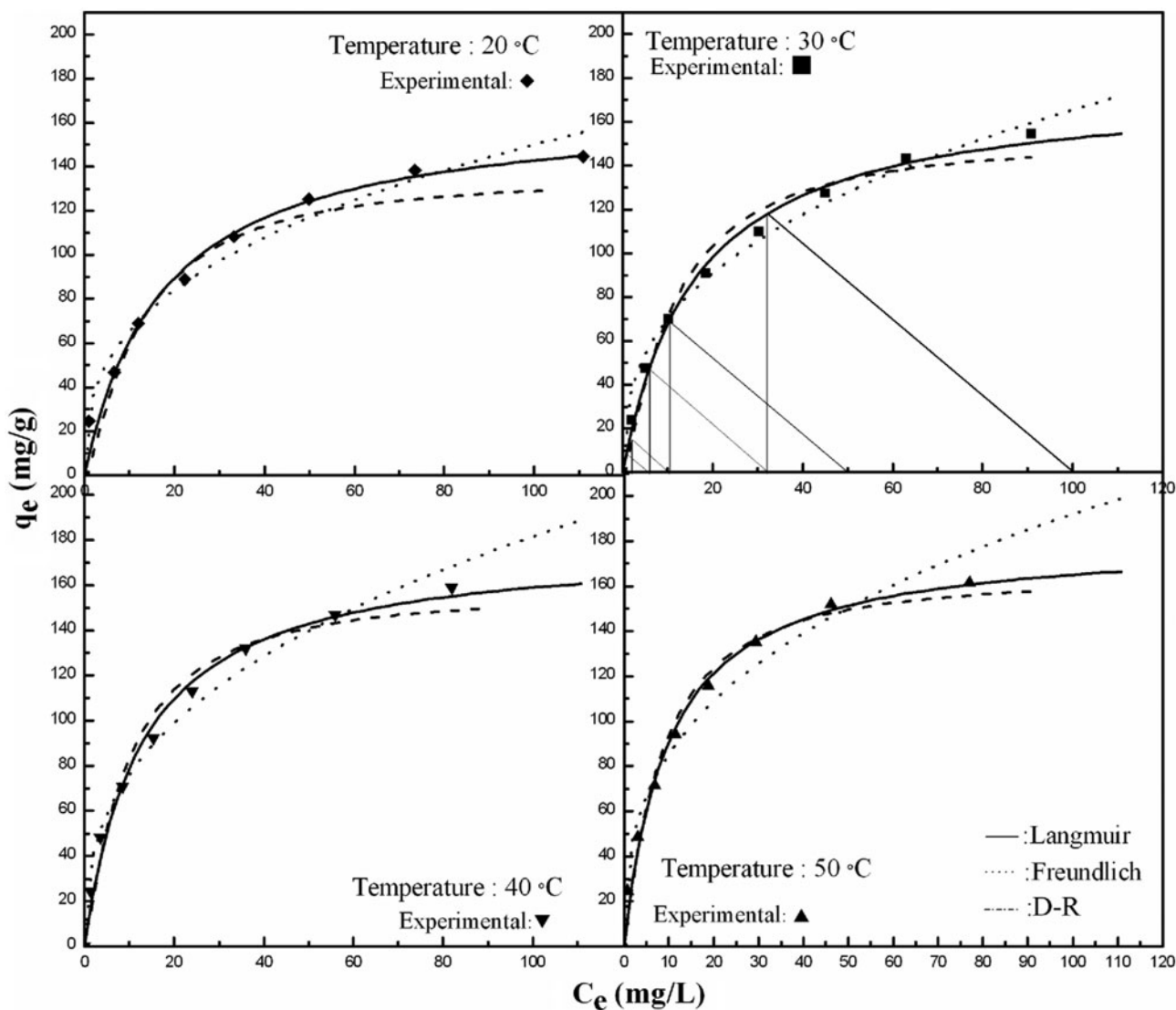


Fig. 8. Comparison of the experimental and model fits of Langmuir, Freundlich and *D*–*R* isotherm plots for the adsorption of Pb(II) onto GA-C-ENCS and the operating lines illustrates the counter current stages.

where  $K_F$  is the Freundlich adsorption constant, which is a comparative measure of the adsorption capacity of the adsorbent and  $1/n_F$  is an empirical constant indicates the intensity of the adsorption. The magnitude of the  $n_F$  gives an indication of the favorability of the adsorbent/adsorbate system. The values of  $n_F$  for GA-C-ENCS are less than unity at all temperatures, indicating high adsorption potential. The values of  $K_F$  increased with increase in temperature from 20 to 50 °C. The decreasing tendency of  $n_F$  indicates that temperature enhances the sorption capacity. It appears that the Freundlich model gives much poorest fit compared to Langmuir model by comparing the  $\chi^2$  values in Table 3. Langmuir and Freundlich isotherms do not

give any idea about sorption mechanism. In order to further assess the different isotherms and their correlation with experimental results, the theoretical plots obtained from each isotherm analysis is shown along with the experimental data for the sorption of metal ions such as Pb(II) onto GA-C-ENCS in Fig. 8.

The *D*–*R* isotherm model was also employed to describe the adsorption data. The *D*–*R* isotherm is more general than the Langmuir isotherm since it does not assume a homogenous surface or constant sorption potential. It was applied to distinguish between the physical and chemical adsorption of metal ions. This nonlinear *D*–*R* isotherm is generally expressed as:

Table 3

Langmuir, Freundlich, and D–R isotherm constants for the sorption of Pb(II) onto GA-C-ENCS

Temperature (°C)	Langmuir				Freundlich			
	Q <sub>0</sub> (mg/g)	b (L/mg)	R <sup>2</sup>	χ <sup>2</sup>	K <sub>F</sub> (mg/g)	n	R <sup>2</sup>	χ <sup>2</sup>
20	145.76	0.04	0.99	1.31	32.12	4.81	0.95	9.31
30	150.94	0.07	0.98	2.12	38.64	3.12	0.93	11.24
40	158.43	0.12	0.98	2.14	58.23	2.87	0.94	14.26
50	166.75	0.16	0.99	1.02	67.25	2.12	0.93	15.32
	D–R							
	q <sub>m</sub> (mg/g)	β × 10 <sup>-3</sup> (mol <sup>2</sup> /kJ <sup>2</sup> )	E (kJ/mol)	R <sup>2</sup>	χ <sup>2</sup>			
20	147.23	3.9	9.89	0.95	6.22			
30	153.21	4.1	12.25	0.98	4.23			
40	162.24	3.4	13.09	0.95	7.61			
50	171.25	3.1	14.26	0.97	3.25			

$$q_e = q_m \exp\left(-\beta \left[RT \ln\left(1 + \frac{1}{C_e}\right)\right]^2\right) \quad (9)$$

where  $q_m$  is the theoretical saturation capacity and  $RT \ln(1 + (1/C_e))$  is the Polanyi potential,  $R$  ( $\text{J mol}^{-1} \text{K}^{-1}$ ) is the gas constant, and  $T$  (K) is the absolute temperature. The constant  $\beta$  is interpreted as the mean free energy of sorption per mole of the sorbate as it is transferred to the surface of the solid from infinite distance in the solution and can be computed using the following relationship:

$$E = \frac{1}{\sqrt{2\beta}} \quad (10)$$

The numerical values of sorption energy ( $E$ ) of adsorption of Pb(II) onto GA-C-ENCS was calculated from the D–R isotherm are in the range of 9–16 kJ/mol and are expected for chemisorption [25]. Hence, it is very likely that the all metal ions are sorbed on GA-C-ENCS, predominantly by chemisorption. The chelating effect of amine functional groups on GA-C-ENCS takes part in the sorption process and chemisorption was found to be the rate-determining step. Both the simulations and  $\chi^2$  values suggest that Langmuir isotherm model described the equilibrium adsorption data better than Freundlich and D–R isotherm models. Fitting of Langmuir isotherm indicates the involvement of interactions between metal ions and homogenous reaction sites on the surface of the adsorbent during the Pb(II) adsorption process. The increase in temperature enhances the sorption, it was also observed in all isotherm curves which indicate

the contribution of stronger binding sites at higher temperature conditions.

### 3.6. Thermodynamic study

The variation in the extent of adsorption with respect to temperature explained on the basis of thermodynamic parameters such as changes in standard free energy ( $\Delta G^\circ$ ), enthalpy ( $\Delta H^\circ$ ) and entropy ( $\Delta S^\circ$ ). These parameters were calculated using the following equations:

$$\Delta G = -RT \ln b \quad (11)$$

$$\ln b = (-\Delta H^\circ/RT + \Delta S^\circ/R) \quad (12)$$

where  $R$  is the gas constant,  $T$  is the temperature on the absolute scale, and  $b$  is the Langmuir constant. From the slope and intercept values of the linear plot of  $\ln b$  vs.  $1/T$ , the values of  $\Delta H^\circ$  and  $\Delta S^\circ$  can be obtained. The observed  $\Delta G^\circ$  values for the adsorption were found to be -21.98, -24.14, -26.34, -27.95 kJ/mol for Pb(II) at 20, 30, 40, and 50°C, respectively.

The negative and small values of  $\Delta G^\circ$  indicate the spontaneous nature of adsorption process. The positive value of  $\Delta H^\circ$  (37.08 kJ/mol for Pb(II)) indicates the endothermic nature of adsorption process. The moderate values obtained in the present study suggest that the adsorption takes place primarily through weak physical forces and chemical interaction between the adsorbate and adsorbent. The negative value of  $\Delta G^\circ$  observed at all temperatures reveal the spontaneity of sorption. The results also show that  $[\Delta H^\circ] < [T\Delta S^\circ]$  at all temperatures. This indicates that the adsorption

process is dominated by entropic rather than enthalpic changes.

The heat of adsorption with its variation with surface coverage/loading can provide useful information concerning the nature of the surface of adsorbent and adsorbed species. The heat of adsorption determined for a constant amount of adsorbed sorbate is known as the isosteric heat of adsorption ( $\Delta H_x$ ) and is calculated using Clausius–Clapeyron equation:

$$\frac{d(\ln C_e)}{dt} = \frac{-\Delta H_x}{RT^2} \quad (13)$$

In  $C_e$  vs.  $1/T$  plots for different amounts of Pb(II) loading onto GA-C-ENCS were found to be almost linear and the values of  $\Delta H_x$  were calculated from the slopes of the plots. The values of  $\Delta H_x$  were calculated from the plot of  $\ln C_e$  vs.  $1/T$  for different surface loadings. The values were found to be +20.89, +21.27, +22.10, +21.33, and +22.01 kJ/mol for Pb(II) sorption onto GA-C-ENCS. The significant variation of  $\Delta H_x$  values with surface loading indicates that the GA-C-ENCS used the energetically homogenous surface for the sorption process.

### 3.7. Effect of adsorbent dose and industrial wastewater study

The suitability of the GA-C-ENCS for wastewater treatment was tested by treating it with different industrial wastewater samples collected from battery manufacturing industries situated in Cochin city (India) contains Pb(II) ion. The study of aforementioned analysis was illustrated in Fig. 9. The wastewater sample was characterized by standard methods (APHA, 1992). The effect of adsorbent dose on Pb(II) removal was studied using these real and simulated wastewater samples and the results were illustrated in Fig. 9. Quantitative removal of Pb(II) (99.8%) from 1.0 L of wastewater containing 4.5 mg/L Pb(II) in the presence of several other ions an adsorbent dosage of 0.5 g/L at pH 6.0 and 30°C. It is therefore reasonable to conclude that GA-C-ENCS can be used as an alternative adsorbent for treating wastewater rich in Pb(II) ion. Similarly, the effect of sorbent dose toward Pb(II) was studied and solution containing this metal ion concentration was increased by spiking the real wastewater composition. Quantitative removal of Pb(II) in the water samples having concentration of metal ions of 100 mg/L and wastewater require 2.0 g/L of GA-C-ENCS for the complete removal of Pb(II) ion. Comparison of sorption potential between CS and GA-C-ENCS reveals that sorption capacity of GA-C-ENCS increased more than twice as CS.

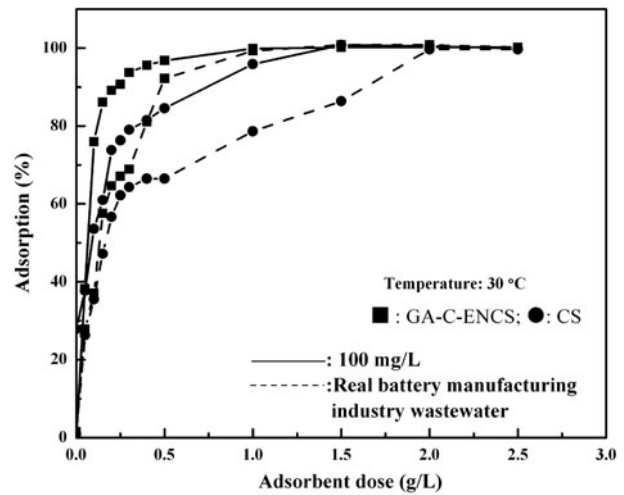


Fig. 9. Variation of the effect of adsorbent dose on the removal of Pb(II) onto GA-C-ENCS.

### 3.8. Batch adsorber design

A schematic diagram for crosscurrent batch design is given in Fig. 10. The design objective is to reduce the solution volume ( $V$ (L)) from an initial concentration  $C_0$  to  $C_n$  mg/L. Initially, when time  $t = 0$ ,  $q = 0$ , the amount of sorbent added is  $m_1$  g, then after “ $n$ ” stages of operation sorbent mass becomes  $m_n$ . The overall mass balance for “ $n$ ” stages was found to be as follows:

$$V(C_{n-1} - C_n) = m(q_{t,n} - q_0) \quad (14)$$

$$\frac{m}{V} = \frac{C_{n-1} - C_n}{q_{t,n} - q_0} \quad (15)$$

A Langmuir isotherm plot at room temperature (30°C) was employed under equilibrium conditions for the process design.

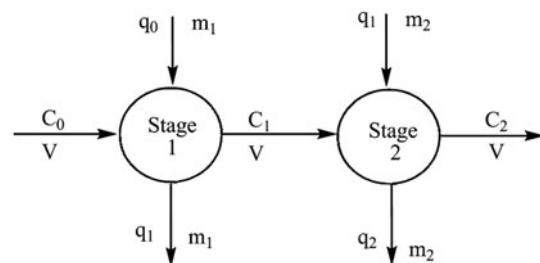


Fig. 10. Schematic representation for a two stage crosscurrent batch adsorption process.

Then Eq. (15) can be rearranged as:

$$\frac{m}{V} = \frac{C_{n-1} - C_n}{q_e} = \frac{C_0 - C_e}{q_e} = \frac{C_0 - C_e}{\frac{Q_0 b C_e}{1 + b C_e}} \quad (16)$$

$$q_e = \frac{Q_0 b C_e}{1 + b C_e} = -\frac{V}{m} C_e + \frac{V}{m} C_0 \quad (17)$$

According to the equation, we could construct the operational lines onto the isotherm curve with a slope ( $V =$  volume of sample in L;  $m =$  mass of adsorbent in g). Fig. 8 also shows the operating lines, which are drawn with a slope of  $-V/m$ . The operating lines connect  $(C_0, q_0)$  to  $(C_e, q_e)$  at equilibrium.

The final equilibrium solution concentration is predicted from the point of intersection of the operating lines on the Langmuir isotherm for the adsorption of Pb(II). The operating line having a slope  $V/m = -0.5$  is drawn through the metal concentrations 50 and 100 mg/L. The corresponding  $q_e$  values obtained from the Langmuir equation and from the operational line are 9.8, and 31.5 mg/g from an initial concentration of 50 and 100 mg/L, respectively, for the periodical recovery of Pb(II).

The operating lines also help in determining the theoretical number of stages for the removal of Pb(II) from aqueous solution. An operating line having a slope  $V/m = -0.5$  was drawn through the initial concentration in solution,  $C_0 = 100$  mg/L and while loading zero mg/g of adsorbent as shown in Fig. 8. The solution treated contain  $L \text{ dm}^3$  solution and the Pb(II) concentration was reduced for each stage from  $C_0$  to  $C_n$  mg/L.

Now the total amount of metal removal can be calculated analytically as follows:

$$\sum_{n=1}^m C_{n-1} - C_n = \sum_{n=1}^m \frac{Q_0 b C_e}{1 + b C_e} \frac{m}{V} \quad (18)$$

Here  $n$  is the adsorption system number ( $n = 1, 2, 3, \dots, m$ ). The Pb(II) removal,  $R_n$  in each stage can be evaluated from the equation as follows:

$$\sum_{n=1}^m R_n = \frac{100(C_{n-1} - C_n)}{C_0} = \frac{100 m Q_0 b C_e}{V C_0 (1 + b C_e)} \quad (19)$$

It was found that Pb(II) concentration was reduced from 100 to 1 mg/L in three stages and the same quantity sorbent requires three stages to reach the discharge limit.

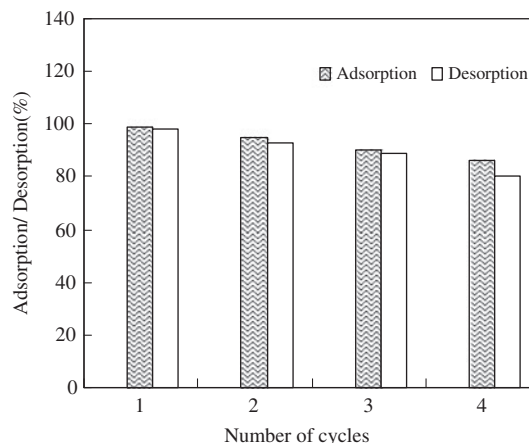


Fig. 11. Four cycles of Pb(II) adsorption-desorption with 0.1 M HCl as the desorbing agent.

### 3.9. Desorption and regeneration studies

Recyclability of an adsorbent is of crucial importance in industrial practice for metal removal from wastewater. To test the suitability and stability of the adsorbent, it was subjected to successive adsorption and desorption cycles. Desorption study was carried out to recover the metal and recycle the adsorbent and treated water. Desorption tests were carried out using different types of 0.1 M desorbing agents such as NaOH,  $\text{Na}_2\text{SO}_4$ , NaCl,  $\text{NaNO}_3$ , HCl, and  $\text{HNO}_3$ . A plot of number of cycles employed for sorption/desorption behavior against the % removal was ascribed in Fig. 11. The percentage desorption of Pb(II) for NaOH,  $\text{Na}_2\text{SO}_4$ , NaCl,  $\text{NaNO}_3$ , HCl, and  $\text{HNO}_3$  was 56.3, 61.4, 62.9, 66.3, 96.0, and 82.1%, respectively.

Among these reagents, 0.1 M HCl was proved to be the most suitable desorbing reagent for the recovery of Pb(II). The feasibility of the adsorption-desorption cyclic operation was examined to check out the long-term performance of the adsorbent. The recovery of Pb(II) ion in 0.1 M HCl decreased from 98.9 to 87.8% in the first cycle to in the fourth cycle. Adsorption-desorption operations illustrating stabilized performance of the sorbent in repeated cycles.

## 4. Conclusions

The capability of a newly developed adsorbent GA-C-ENCS for removing Pb(II) was examined under various experimental conditions. FTIR, SEM-EDS, XPS, and potentiometric titration were used to characterize the adsorbent. Sorption of Pb(II) was pH dependent and more than 99.0% removal was achieved at pH 6.0. The kinetics of the sorption process was found to

follow the pseudo-second-order rate law and the response time evaluation was done using reversible-first-order rate law. The adsorption increases with increasing temperature. The isotherm data were correlated well by Langmuir model as compared to D-R and Freundlich isotherm models. Adsorbent exhibited high adsorption capacity, the maximum adsorption capacity for Pb(II) was 150.94 mg/g 30°C. D-R isotherm parameters indicate the energetically heterogeneous sites on the surface of the adsorbent. Quantitative removal of 4.5 mg/L Pb(II) in 1.0 L of battery manufacturing industry wastewater require 0.5 g GA-C-ENCS indicate the robust nature of sorbent over matrix ions. An adsorption–desorption study also elucidates the consistent long-term performance of sorbent.

## References

- [1] A. Celik, A. Demirbaş, Removal of heavy metal ions from aqueous solutions via adsorption onto modified lignin from pulping wastes, *Energy Sources* 27 (2005) 1167–1177.
- [2] S. Tunali, T.A. Akar, A.S. Özcan, I. Kiran, A. Özcan, Equilibrium and kinetics of biosorption of lead(II) from aqueous solutions by *Cephalosporium aphidicola*, *Sep. Purif. Technol.* 47(3) (2006) 105–112.
- [3] M. Nadeem, A. Mahmood, S.A. Shahid, S.S. Shah, Sorption of lead from aqueous solution by chemically modified carbon adsorbents, *J. Hazard. Mater.* 138(3) (2006) 604–613.
- [4] S.G. Wang, W.X. Gong, X.W. Liu, Y.W. Yao, B.X. Gao, Q.Y. Yue, Removal of lead(II) from aqueous solution by adsorption onto manganese oxide-coated carbon nanotubes, *Sep. Purif. Technol.* 58 (2007) 3551–3556.
- [5] USEPA, National Primary Drinking Water Regulations for Lead and Copper: Short-Term Regulatory Revisions and Clarifications, *Fed. Register* 72 (2007) 57782–57820.
- [6] J. Demirbas, Heavy metal adsorption onto agro-based waste materials: A review, *J. Hazard. Mater.* 157 (2008) 220–229.
- [7] B.L. Rivas, B. Quilodrán, E. Quiroz, Trace metal ion retention properties of crosslinked poly(4-vinylpyridine) and poly(acrylic acid), *J. Appl. Polym. Sci.* 92 (2004) 2908–2916.
- [8] E. Ramírez, S.G. Burillo, C. Barrera-Díaz, G. Roa, B. Bilyeu, Use of pH-sensitive polymer hydrogels in lead removal from aqueous solution, *J. Hazard. Mater.* 192 (2011) 432–439.
- [9] E. Piron, M. Accominoti, A. Domard, Interaction between chitosan and uranyl ions. Role of physical and physicochemical parameters on the kinetics of sorption, *Langmuir* 13(6) (1997) 1653–1658.
- [10] E. Guibal, M. Jansson-Charrier, I. Saucedo, P. Cloirec, Enhancement of metal ion sorption performances of chitosan: Effect of the structure on the diffusion properties, *Langmuir* 11(2) (1995) 591–598.
- [11] V.M. Boddu, K. Abburi, J.L. Talbott, E.D. Smith, R. Haasch, Removal of arsenic(III) and arsenic(V) from aqueous medium using chitosan-coated biosorbent, *Water Res.* 42 (2008) 633–642.
- [12] K.C. Justi, V.T. Fávere, M.C.M. Laranjeira, A. Neves, R.A. Peralta, Kinetics and equilibrium adsorption of Cu(II), Cd(II), and Ni(II) ions by chitosan functionalized with 2[-bis-(pyridylmethyl)aminomethyl]-4-methyl-6-formylphenol, *J. Colloid Interface Sci.* 291 (2005) 369–374.
- [13] S.C. Hsu, T.M. Don, W.Y. Chiu, Free radical degradation of chitosan with potassium persulfate, *Polym. Degrad. Stab* 75 (2002) 73–83.
- [14] J.A. Schwarz, C.T. Driscoll, A.K. Bhanot, The zero point of charge of silica—Alumina oxide suspensions, *J. Colloid Interface Sci.* 97 (1984) 55–61.
- [15] A.K. Roy, S.K. Sen, S.C. Bag, S.N. Pandey, Infrared spectra of jute stick and alkali-treated jute stick, *J. Appl. Polym. Sci.* 42(11) (1991) 2943–2950.
- [16] J.F. Moulder, W.F. Stickle, P.E. Sobol, K.D. Bomben, in: J. Chastain (Ed.), *Handbook of X-Ray Photoelectron Spectroscopy*, Perkin Elmer, Eden Prairie, MN, 1992.
- [17] L. Hernán, J. Morales, J. Santos, J.P. Espinós, A.R. González-elipe, Preparation and characterization of diamine intercalation compounds of misfit layer sulfides, *J. Mater. Chem.* 8(10) (1998) 2281–2286.
- [18] L.R. Pederson, Two-dimensional chemical-state plot for lead using XPS, *J. Electron. Spectrosc. Relat. Phenom.* 28 (1982) 203–209.
- [19] S.M. Lee, A.P. Davis, Removal of cu(II) and cd(II) from aqueous solution by seafood processing waste sludge, *Water Res.* 35 (2001) 534–540.
- [20] K. Ndungu, M.P. Hurst, K.W. Bruland, Comparison of copper speciation in estuarine water measured using analytical voltammetry and supported liquid membrane techniques, *Environ. Sci. Technol.* 39 (2005) 3166–3175.
- [21] V.M. Nurchi, I. Villaescusa, Sorption of toxic metal ions by solid sorbents: A predictive speciation approach based on complex formation constants in aqueous solution, *Coord. Chem. Rev.* 256(1–2) (2012) 212–221.
- [22] R. Herrera-Urbina, D.W. Fuerstenau, The effect of Pb(II) species, pH and dissolved carbonate on the zeta potential at the quartz/aqueous solution interface, *Colloids Surf., A* 98 (1995) 25–33.
- [23] V.K. Gupta, S.K. Srivastava, D. Mohan, Equilibrium uptake, sorption dynamics, process optimization, and column operations for the removal and recovery of malachite green from wastewater using activated carbon and activated slag, *Ind. Eng. Chem. Res.* 36 (1997) 2207–2218.
- [24] A. Turner, M. Crussell, G.E. Millward, A.C. Cobelo-Garcia, A.S. Fisher, Adsorption kinetics of platinum group elements in river water, *Environ. Sci. Technol.* 40 (2006) 1524–1531.
- [25] S.Q. Memon, S.M. Hasany, M.I. Bhangar, M.Y. Khuhawar, Enrichment of Pb(II) ions using phthalic acid functionalized XAD-16 resin as a sorbent, *J. Colloid Interface Sci.* 291 (2005) 84–91.